Conduction in alumina with atomic scale copper filaments

Xu Xu, Jie Liu, and M. P. Anantram
Department of Electrical Engineering, University of Washington, Seattle, Washington 98195, USA

(Received 30 June 2014; accepted 2 October 2014; published online 22 October 2014)

The conductance of atomic scale filaments with three and seven Cu atoms in α-alumina are calculated using *ab initio* density functional theory. We find that the filament with 3 Cu atoms is sufficient to increase the conductance of 1.3 nm thick alumina film by more than 10^3 times in linear response. As the applied voltage increases, the current quickly saturates and differential resistance becomes negative. Compared to the filament with three Cu atoms, while the conductance of the filament with seven Cu atoms is comparable in linear response, they carry as much as twenty times larger current at large biases. The electron transport is analyzed based on local density of states, and the negative differential resistance in the seven Cu filaments occurs due to their narrow bandwidth. © *2014 AIP Publishing LLC*. [http://dx.doi.org/10.1063/1.4898073]

I. INTRODUCTION

A number of metal oxides have shown the possibility to reversibly switch between high and low resistivity states via the forming and rupture of conductive filaments. The switching behavior usually can be found in pervoskite oxides of $SrTiO_3$, $SrZrO_3$, or binary metal oxides such as NiO, TiO_2, HfO_x, or AlO_x, which are good insulators in the crystalline state. Although the detailed understanding of the switching mechanism is still lacking, there are several widely accepted mechanisms to explain the characteristics, including charge trapping, conductive filament formation, electrochemical migration of point defects and others.[1–4] In general, these mechanisms conclude that defects, such as interstitial metal atoms or oxygen vacancies, can change the resistivity of the insulator in a small area, and a conductive filament forms and ruptures by moving and forming these defects. An important application of the atomic scale filaments embedded in metal oxides is the switching layer in resistive memory (ReRAM) devices. In conventional Flash memory, the logic states 0 and 1 are stored by the electrons in a floating gate. Electron tunneling out of the floating gate results in loss of information in deeply scaled Flash memory. In contrast, the resistive memory stores information by the presence or absence of tiny conductive filaments, in a switching material, which can be reversibly controlled by applying an external voltage. Since the mass of an atom is much larger than the mass of an electron, the filaments are more stable, and thereby the logic states are retained over longer time periods. The resistive memory devices have a potential for longer endurance, faster response, and lower energy consumption compared with non-volatile Flash memory.[5–21]

A number of experimental studies use alumina in resistive switching.[22–32] Alumina is a desirable material because it has a large band gap and as a result the leakage current is small. Experimentally, it has been shown that the leakage current in a 1.2 nm alumina film is smaller than 10^{-4} A/cm^2.[33] Also, the deposition of alumina using atomic layer deposition (ALD) is well studied and compatible with the advanced CMOS technology. Unipolar ReRAMs based on alumina have been reported in Ref. 29, and bipolar ReRAM with a cross-bar structure has also reported in Ref. 30. The RESET current reported in experiments can be as low as 1 μA. Several groups have also studied a switching layer consisting of alumina stacked with other oxides.[31,32] Therefore, alumina is a promising candidate as the switching layer in ReRAM. Metallic filaments can be formed in alumina by interstitial Cu defects. In this paper, we study the device physics of electron transport in metal-insulator-metal (MIM) configuration, where the insulator is alumina and the metal electrodes are copper. Our focus is to understand the conductance with and without Copper atoms in the interstitials of alumina. Because the transport property is dominated by the insulator layer, we choose both electrodes as copper to simplify the problem.

We believe that such a study will yield insights into the smallest filaments that are capable to change the resistance of alumina appreciably and contribute to the understanding of the scaling properties of resistive memory devices. Our results reveal that a few Cu atoms in Al_2O_3 can change the resistivity by about a thousand times at low biases. We also discuss the saturation of current and negative differential resistance (NDR) that emerge with increase in bias.

II. METHOD

The atomic positions of Al_2O_3 are obtained by variable-cell relaxation of the hexagonal $2 \times 2 \times 1$ α-Al_2O_3 lattice, which has 120 atoms per unit cell. Using the conjugate gradient (CG) algorithm with periodic boundary condition, the Feynman-Hellmann forces on all atoms in the unit cell are less than 0.02 eV/Å, and the pressure on the unit cell is less than 1 GPa. We obtain lattice constants of a = 4.7572 Å, c = 13.0834 Å, which are close to the experimental values of a = 4.7591 Å, c = 12.9894 Å.[34] The calculated bandgap of Al_2O_3 is 6.0 eV, which is smaller than the experimental bandgap of 8.8 eV.[35]

We first determine the interstitial sites in Al_2O_3 where a Cu atom can reside. The crystal structure has a number of hollow positions, which can serve as an interstitial site for Cu atoms. We have calculated the formation energy of these interstitials and the results are summarized in the Appendix A. In α-Al_2O_3, the Al atoms form a chain in the (0001) direction

 © 2014 AIP Publishing LLC

[This article is copyrighted as indicated in the article. Reuse of AIP content is subject to the terms at: http://scitation.aip.org/termsconditions. Downloaded to] IP: 128.95.215.214 On: Thu, 06 Nov 2014 19:31:09

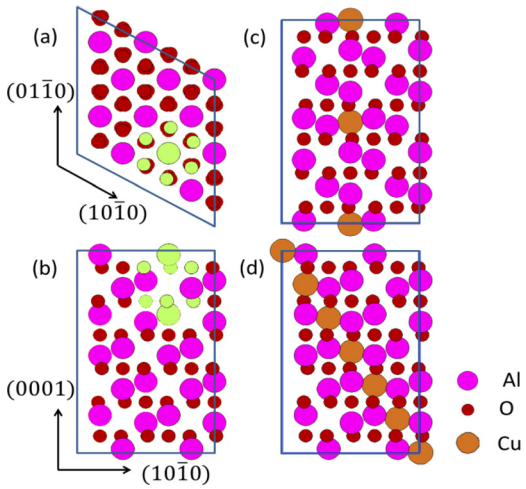


FIG. 1. The structure of α-Al_2O_3 in a hexagonal unit cell viewed along the (a) (0001) and (b) (1$\bar{1}$01) directions. The two Al and six O atoms highlighted in green enclose an interstitial for a Cu atom. (c) 3 Cu atom filament along the (0001) direction. (d) 7 Cu atom filament along the (1$\bar{1}$01) direction.

with alternating separations of 2.674 Å and 3.875 Å as shown in Figure 1. The lowest energy interstitial is encompassed by two Aluminum atoms separated by 3.875 Å along the (0001) direction and two layers of oxygen atoms each consisting of three atoms as shown in Fig. 1(a). The relaxation gives the energy minimized structure with the constraint that the lattice parameters are the same as pure Al_2O_3, and local strain within this constraint is naturally included. We consider two atomic filaments of Cu inside Al_2O_3. The first atomic filament considered has 3 Cu atoms that fill the interstitial sites along the (0001) direction, and the separation between Cu atoms equals to 6.549 Å (Fig. 1(c)). Note that in this structure, there are two aluminum atoms between the consecutive copper atoms in the (0001) direction. The second filament considered has 7 Cu atoms in the (1$\bar{1}$01) direction, with the 3.25 Å separation between Cu atoms (Fig 1(d)). The distances between two atomic filaments in the 3-Cu atom and 7-Cu atom cases are 9.514 Å and 6.958 Å, respectively. We would like to emphasize that while we have relaxed these structures using energy minimization, these filament configurations do not emerge from *ab initio* molecular dynamics simulations, which is extremely difficult for these large system sizes. Our intent here is to gain insight into the device physics for idealized filament configurations where the Cu atoms are placed in well-defined locations without any randomness, as shown in Figures 1(c) and 1(d).

An ultrathin layer of Al_2O_3 that is one lattice constant thick (1.31 nm) is sandwiched by two Cu electrodes in our model. We note that even such a calculation is computationally challenging because we include a total of 360 atoms (aluminum, oxygen and copper). However, there has been experimental work involving thin oxide layers. Reference 33 measured very small leakage currents in 1.2 nm thick alumina. Further, experiments on resistive memory have demonstrated successful reversible switching in oxides (GdO_x) of thickness of 2 nm (Ref. 36) with a lateral feature size of 40 nm. Recently, Ref. 28 has also demonstrated switching in alumina with thickness of 3 nm.

We note that the surface of alumina on the (0001) planes forms a hexagonal lattice with a lattice constant of 9.52 Å (Fig. 2(a)). On the other hand, fcc Copper with a lattice constant of 3.61 Å also has a hexagonal lattice in the (111) plane. The precise interface between Al_2O_3 and the copper contacts would depend on the experimental method for fabrication. This is a difficult problem in itself and here we are guided by Refs. 37–39, which has studied the energy favorable contact between Al_2O_3 and Cu. We stretch the Cu lattice by 6.9% in the (111) plane to make the lattice constants of both Al_2O_3 and Cu at the metal-oxide interface identical.[24] Note that Cu remains metallic with no major changes.

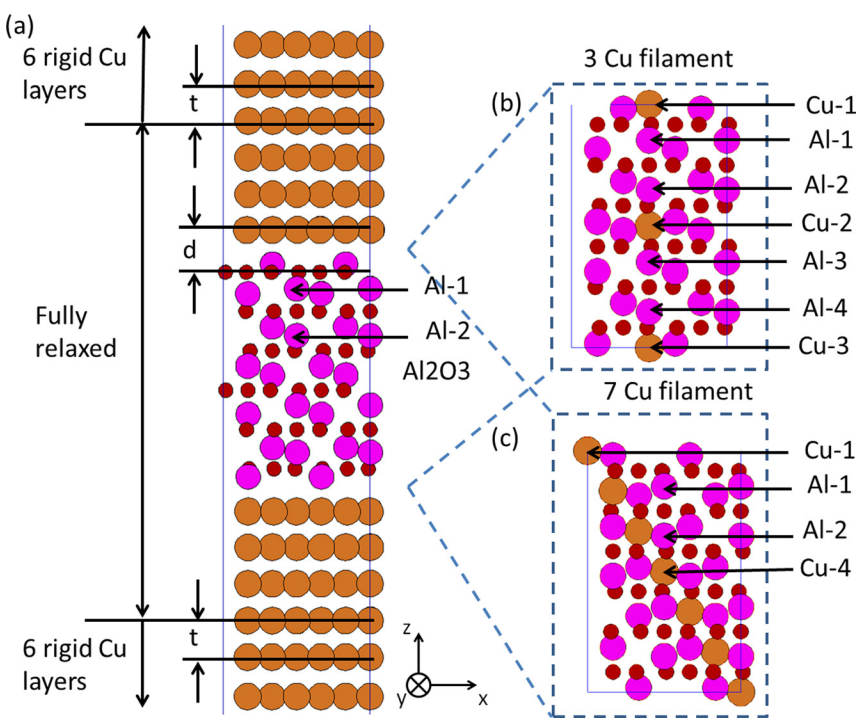


FIG. 2. MIM simulation models in which alumina without, with 3-Cu atom, and with 7-Cu atom filaments are shown in (a), (b) and (c) respectively. Periodic boundary conditions (PBC) are applied in the (x, y) plane. For clarity, only two out of the six rigid layers of Cu atom are shown in the figure.

[This article is copyrighted as indicated in the article. Reuse of AIP content is subject to the terms at: http://scitation.aip.org/termsconditions. Downloaded to] IP: 128.95.215.214 On: Thu, 06 Nov 2014 19:31:09

For the electrode-alumina configuration, we first note that Al-ended Al_2O_3 is widely accepted as the most stable surface structure when exposed to vacuum. The O-top structure of Cu-Al_2O_3 contact is the most stable structure.[37–40] In the O-top structure, the Cu atoms sit directly on top of the first layer of O atoms near the interface. Our procedure for energy minimization of the O-top structure involves a full relaxation of a periodic structure consisting of four layers of Cu at each end of the Al_2O_3 as shown in Fig. 2(a), with an initial Cu-O distance of 3.25 Å (distance d in Fig. 2(a)). We then attach a rigid structure consisting of six Cu layers (with an interlayer distance equal to 2.11Å), and perform a constrained energy relaxation where distance t shown in Fig. 2(a), can vary. The purpose of the outer six copper layers is to mimic crystalline copper, using which we will obtain the open boundary conditions to calculate the transport properties. Finally, a single point density functional theory (DFT) calculation on the entire structure consisting of Al_2O_3 and a total of twenty Cu layers is performed to obtain the Hamiltonian (**H**) and overlap (**S**) matrices of the MIM structures in the pseudo atomic orbital (PAO) basis. The Hamiltonian and overlap matrices given by DFT calculations have tiny portions of non-Hermitian and non-symmetric components because of numerical errors. We symmetrized these matrices by $H \leftarrow (H + H^{\dagger})/2$, and $S \leftarrow (S + S^{T})/2$ to avoid numerical errors.

The CG and DFT calculations are performed using the SIESTA package[41] with a Γ-point sampling since the unit cell is large; the plane wave cutoff is 200 Ry; the generalized gradient approximation (GGA) of Perdew, Burke, and Ernzerhof (PBE)[42] is used to estimate the exchange-correlation energy; the CG relaxation force threshold is set as 0.02 eV/Å. The single-zeta plus polarization (SZP) PAO is used for all atoms during relaxation since CG calculations with double-zeta polarized (DZP) is oppressive. However, all electronic structure calculations, including transmission, density of states, and current-voltage characteristics, are performed using the DZP PAO for the scattering region and SZP for the electrodes.[43]

The transport properties of Al_2O_3 with and without Cu atoms are calculated using the equations described below. Note that while scattering due to various interfaces and the presence of Cu atoms in Al_2O_3 are included, our calculations do not account for decoherence. The transmission for electrons with energy E is given by

$$T(E,V) = Tr[\Gamma_T(E,V)G^r(E,V)\Gamma_B(E,B)G^a(E,V)].$$

Here,

$$G^r(E,V) = [ES - V - H - \Sigma_T(E,V) - \Sigma_B(E,V)]^{-1}$$

is the retarded Green's function, $\Sigma_{T/B}$ are self-energies of the top/bottom electrodes, which are constructed from the outer six Cu atom layers of Fig. 2(a). T and B refer to top and bottom electrodes, respectively. In the presence of a voltage bias, the electrostatic potential (φ) is assumed to drop linearly along the z-direction in alumina. Thus the term $V = q\varphi$ corresponding to the electrostatic potential energy due to the external voltage drop is added to the Hamiltonian. The broadening matrices are given by

$$\Gamma_{T/B}(E,V) = i[\Sigma_{T/B}(E,V) - \Sigma^{\dagger}_{T/B}(E,V)].$$

The retarded Green's function naturally contains information that describes the scattering process. The orbital-resolved local density of states (LDOS) can be calculated as, $LDOS_O(n,E,V) = -\frac{1}{\pi}\mathrm{Im}(G^r_{nn}(E,V))$, where $G^r_{nn}(E,V)$ is the nth diagonal element of matrix $G^r(E,V)$. The LDOS on atom i is the summation of orbital-resolved LDOS over the atom, $LDOS_A(i,E,V) = \Sigma_{n\in\{atom\,i\}}\ LDOS_O(n,E,V)$. Here, $\{atom\ i\}$ refers to the set of orbitals centered at the ith atom. The current-voltage relation is calculated using

$$I(V) = \frac{2q^2}{h}\int T(E,V)[f(E - V/2) - f(E + V/2)]dE,$$

where $f(E)$ is the Fermi function at temperature 300 K.

III. RESULTS

A. Transmission coefficient at zero bias

To understand how atomic scale Cu filaments affect the conductivity of Al_2O_3 film, we present the transmission of electrons in the case of pure Al_2O_3, and the film with three and seven Cu atom filaments. For pure Al_2O_3, the tunneling probability through the 1.3 nm thick oxide is small at the Fermi energy (blue curve of Fig. 3) because of the large bandgap. With the 3-Cu and 7-Cu atom filaments, the interstitial Cu atoms in the oxide create energy levels within the oxide bandgap, which increase the transmission significantly (red and green curves of Fig. 3). Our calculations show that both the 3-Cu atom and 7-Cu atom filaments change the transmission probability at the Fermi energy by over 10^3 times. The 3-Cu atom filament has two peaks in the transmission spectrum, and the transmission window width is approximately 0.12 eV while the 7-Cu atom filament has a wider transmission window approximately 0.2 eV wide. Note that while the peak transmission is close to unity as expected in a wide-narrow-wide geometry,[44] the transmission at the Fermi energy is smaller than unity. As a result, the linear response conductance is smaller than the quantum of conductance

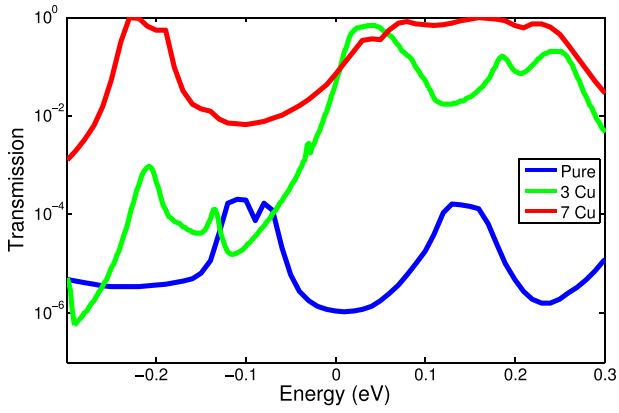


FIG. 3. Transmission spectrum for pure Al_2O_3 and the structures doped with 3 Cu atom and 7 Cu atom filaments. The energy axis is shifted that the zero of energy is the Fermi energy at equilibrium.

[This article is copyrighted as indicated in the article. Reuse of AIP content is subject to the terms at: http://scitation.aip.org/termsconditions. Downloaded to] IP: 128.95.215.214 On: Thu, 06 Nov 2014 19:31:09

$2q^2/h$, and low bias resistance is larger than 12.9 kΩ. The linear response resistances (R) calculated using

$$R^{-1} = G = \frac{2q^2}{h}\int T(E)\frac{df(E)}{dE}dE$$

are 306.9 MΩ, 78.37 kΩ, and 96.56 kΩ for pure alumina, and the 3-Cu and 7-Cu atom filaments, respectively. This implies that the diffusion of just a few Cu atoms can cause a huge change in the linear response resistance.

The analysis of LDOS provides further insight. We plot the LDOS at five atoms to determine the conducting path: Cu-1 (Cu atom near the left electrode), Al-1 and Al-2 (Al atoms in alumina), Cu-2 (Cu atom in the middle of the 3-Cu atom filament), and Cu-4 (Cu atom in the middle of the 7-Cu atom filament). As shown in Fig. 4(a), we observe that for pure alumina, the metal induced gap states penetrate into the pure alumina. However, the transmission is still low near Fermi level because LDOS on Al-2, which is furthest away from the electrodes, has a small value. Thus, the low transmission results in high resistance in the OFF state, and therefore leads to high OFF/ON resistance ratio. On the other hand, atom Al-2 has a much higher LDOS in the 3-Cu atom filament because of close proximity to the filament (Figs. 4(b) and 4(c)), which causes the higher conductance. The conductive path for 3-Cu atom filament is along (0001) direction since atom Al-1 also has a large LDOS in the 3-Cu filament (Fig. 4(b)). Further analysis shows that the m = 0 orbitals primarily contribute to the LDOS around the Fermi level to form the conductive path (see Appendix B for detail). In comparison, the conductive path in the 7-Cu filament is along the $(1\bar{1}01)$ direction. The LDOS on the aluminum atom (Al-2) is similar to the 3-Cu atom filament case since it is close to the Cu filament, while the LDOS is much smaller on Al-1 atom because it is located further away from the Cu-atom filament (Fig. 4(c)). To sum up, Cu atoms in Al_2O_3 increases the LDOS of atoms nearby, which aid to form the conductive path.

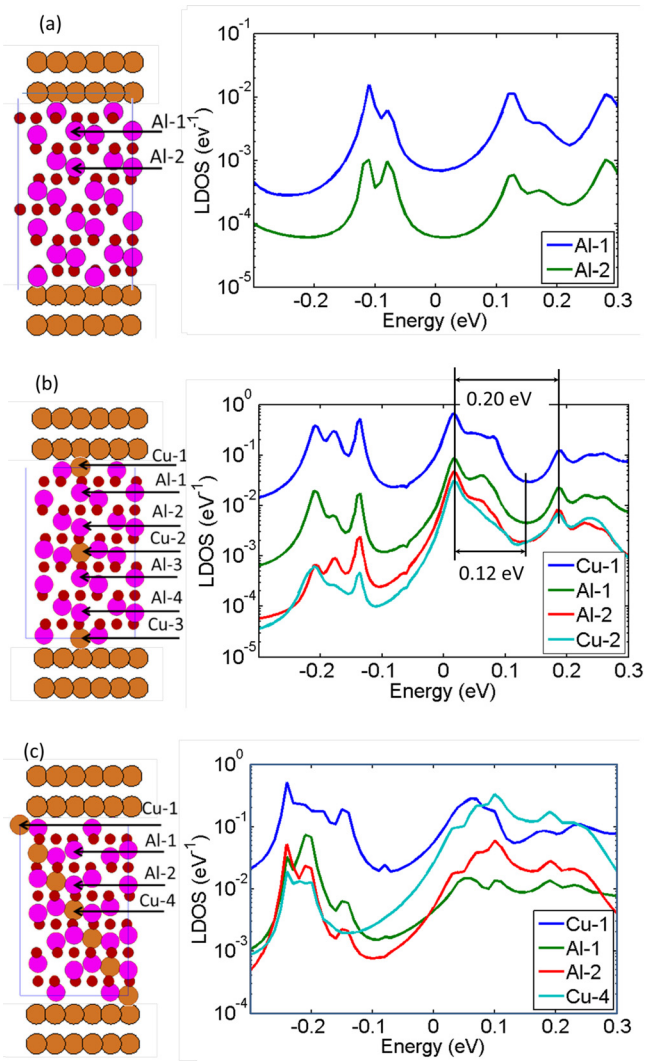


FIG. 4. LDOS for various atoms in the alumina layer for (a) pure alumina, (b) alumina with the 3-Cu atom filament and (c) alumina with the 7 Cu atom filament. LDOS is calculated with electrodes in the MIM structure. We find that the Cu atoms can increase the LDOS of neighboring Al atoms. Note that the energy axis is shifted such that the zero of energy is the Fermi energy at equilibrium.

B. Current-voltage relation

We find that the current is larger for the 3-Cu atom chain when compared to the 7-Cu atom chain at applied biases smaller than 50 mV (Fig. 5), which is in agreement with the above results for linear response resistance. For biases larger than 50 mV, there are three important features: (i) the current in the 3-Cu and 7-Cu atom filaments saturate at biases larger than 50 mV and 0.25 V, (ii) negative differential resistance is observed in both filaments, with it being more pronounced in the 3-Cu atom filament, and (iii) there is a large difference (approximately twenty times) in current between the 3-Cu and 7-Cu atom filaments when the applied bias is in the range of 0.4 V. This result is interesting because it shows that small changes in the filament can give rise to large changes in the features of the current-voltage characteristics. Changing the shape of the filament experimentally is beyond our expertise but we would like to point out that this is being pursued experimentally to investigate if multi-level logic is feasible in the structures considered. Our calculations merely

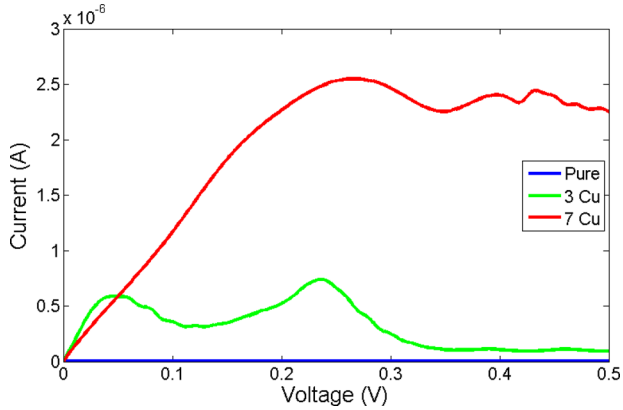


FIG. 5. Current-voltage characteristics of pure alumina and the structures with the 3-Cu and 7-Cu atom filaments. There is a large difference in current between the 3-Cu atom and 7-Cu atom filament cases when the bias is around 0.4 V. Features of negative differential resistance are seen in the current voltage characteristics, which occur due to a mismatch in the LDOS.

[This article is copyrighted as indicated in the article. Reuse of AIP content is subject to the terms at: http://scitation.aip.org/termsconditions. Downloaded to] IP: 128.95.215.214 On: Thu, 06 Nov 2014 19:31:09

points that large changes in the current are possible if there are small changes in the filament. The reason for these features is discussed now. When a voltage is applied, the quasi-Fermi levels on two electrodes shift by $\pm eV/2$, respectively, and the transmission at energies in between the two quasi-Fermi levels contributes to current flow. The reason for current saturation is the narrow transmission window seen in the inset of Fig. 3. The narrower transmission peak in the case of the 3-Cu atom filament causes a current saturation at smaller biases, when compared to the 7-Cu atom filament. The NDR is caused by the mismatch of LDOS along the conductive path. This notion is studied further by looking at the transmission spectrum and LDOS under finite bias for the 3-Cu atom filament. The NDR in the I-V curve emerges from a density of states effect and this should be observable at room temperature (300 K) given that we have atomically narrow filaments. We find that the transmission versus energy has two peaks (green line of Fig. 3 and blue line of Fig. 6). Each peak splits into two sub-peaks when a bias is applied as shown in Fig. 6(a)—while one sub-peak is shifted by $+eV/2$, the other sub peak is shifted by $-eV/2$. The reason for the split in transmission spectrum is that the LDOS of the Cu-1 and Cu-3 are shifted by energies approximately equal to $\pm eV/2$ (Fig. 6(b)) compared to the zero bias case (Fig. 4(b)). The LDOS of Cu-2 has split into two peaks, one induced by the left electrode (shift by $+eV/2$) and the other induced by the right electrode (shift by $-eV/2$). When the LDOS on the different Cu atoms are matched in energy, there is a large current. The current-voltage characteristic in 3-Cu filament case shows a valley at 0.15 V and a second peak at 0.23 eV. Corresponding to these features, in the plot of LDOS (Fig. 4), the peak-to-valley distance is 0.12 eV and peak-to-peak distance is 0.20 eV. When the applied bias is 0.15 V, the LDOS peak on Cu-1 overlaps with the valley on Cu-3, resulting in small current, which explains the negative differential resistance. And, when the applied bias is 0.25 V, the LDOS peak on Cu-1 overlaps with the LDOS peak of Cu-3, which explains the second peak in current. Our physical picture here shows that the negative differential resistance and the second peak in the current-voltage curve correspond to the energy differences in the peak(Cu-1)-valley(Cu-3) and peak(Cu-1)-peak(Cu-3) features seen in the LDOS.

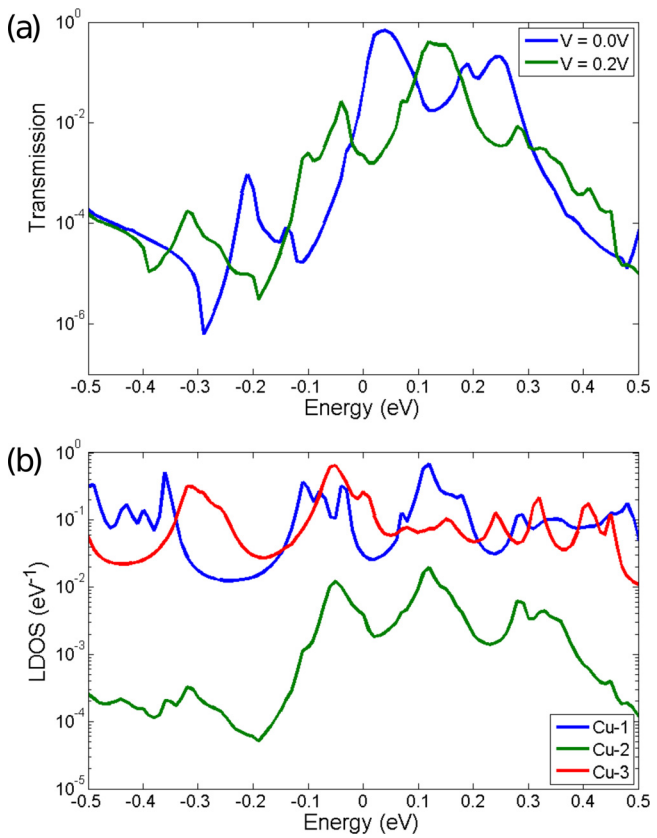


FIG. 6. (a) Transmission spectra of the 3-Cu atom filament under zero bias and a bias of 0.2 Volts; (b) LDOS of the 3-Cu atom filament when the bias is 0.2 V. One can see a split in LDOS by $\pm eV/2$, when a voltage of V is applied.

IV. CONCLUSION

In conclusion, we present the electron transport properties of pure and doped Al_2O_3 using first principle calculations. Our thin film structure consisted of a 1.3 nm thick α-alumina with crystalline copper electrodes. We find that the low bias conductance of crystalline alumina can be changed by more than a thousand times by incorporating few copper atoms in interstitials to form a filament. We show the current of the 3-Cu atom filament saturates at smaller voltages than the 7-Cu atom filament. The current saturates at much higher values in the 7-Cu atom filament, which is consistent with the greater hybridization between Cu atoms as a result of the smaller distance between Cu atoms in the 7-Cu atom filament. This shows that small changes in the filament structure can lead to large changes in the current-voltage characteristic in atomic scale filaments, a conclusion that is of relevance to multi-level logic. We also find that the mismatch in the LDOS at Cu atoms along the filament in the presence of an applied bias leads to a negative differential resistance. Finally, as the conductive behavior is determined by the orbitals of the filament's metal atoms, an *ab initio* study of the optimum metal for filament formation, which can yield an adequate conductance contrast, will be a useful direction for future analysis.

ACKNOWLEDGMENTS

M. P. Anantram and Xu Xu were funded by University of Washington Start Up funds allocated to M. P. Anantram. Jie Liu who developed some of the transport code was funded by U.S. National Science Foundation under Grant 1006182. This work was facilitated through the use of advanced computational, storage, and networking infrastructure provided by the Hyak supercomputer system, supported in part by the University of Washington eScience Institute.

APPENDIX A: INTERSTITIAL POSITIONS IN α-Al_2O_3

In this appendix, we provide details of the various interstitials considered in the alumina lattice, where a Cu atom can reside. Since alumina is a material with high atomic density (1.16×10^{23} per cm^3), it is hard to find locations where

[This article is copyrighted as indicated in the article. Reuse of AIP content is subject to the terms at: http://scitation.aip.org/termsconditions. Downloaded to] IP: 128.95.215.214 On: Thu, 06 Nov 2014 19:31:09

the interstitial defects can reside. We have searched for locations larger than the covalent radius of a Cu atom (1.2 Å) in crystalline Al_2O_3, which can possibly hold interstitial Cu atoms. We test the three most possible locations for interstitial atoms, which are the three farthest positions from Al and O atoms. These positions are described below.

In the hexagonal lattice of α-Al_2O_3, Al atoms form chains in the (0001) direction. The separations between two Al atoms on a chain are 3.82 Å and 2.674 Å. The first interstitial position is shown in Fig. 7(a). It is located at the center of the 3.82 Å separation between Al atoms along the chain in (0001) direction. This position is the hollow site formed in α-Al_2O_3. The nearest neighbors for this interstitial position are two Al atoms, which are located along the (0001) chain and are 1.91 Å away. The second nearest neighbors are the surrounding six O atoms located on two (0001) planes with a separation of 2.12 Å, with the Cu-O distance of 1.97 Å, as shown in the highlighted atoms in Fig. 1(a). Fig. 7(b) shows the second interstitial position, which is along the O atom chain which lies along the (0001) direction. Three O atoms are closest to the interstitial position at a distance of 1.65 Å. And, Fig. 7(c) shows the third interstitial position, which is located on the plane formed by two Al and two O atoms. For this interstitial location, the nearest atoms are O atoms at a separation of 1.31 Å, and the second nearest neighbor atoms are two Al atoms at a distance of 1.39 Å. These three positions are the locations farthest from the atoms in crystalline Al_2O_3 structure, and therefore they are the most possible locations for the interstitial Cu atoms to reside.

We have considered these locations for the Cu atom and have performed energy minimization calculations to determine the most stable location. The formation (E_{form}) energy for the Cu atom is given by

$$E_{form} = E(Al_2O_3 : Cu) - E(Al_2O_3) - E(Cu_{bulk})/64.$$

Here, $E(Al_2O_3{:}Cu)$ is the total energy of 120 atoms in Al_2O_3 with one Cu atom in the interstitial, $E(Al_2O_3)$ is the total energy of the 120 atom unit cell of crystalline Al_2O_3, and $E(Cu_{bulk})$ is the energy of fcc Cu whose unit cell contains 64 atoms. The formation energy for the Cu atom located at the first possible interstitial position described above is 7.92 eV. We find that Cu atoms put in either the second or third positions of the interstitials relax to the position of the first interstitial.

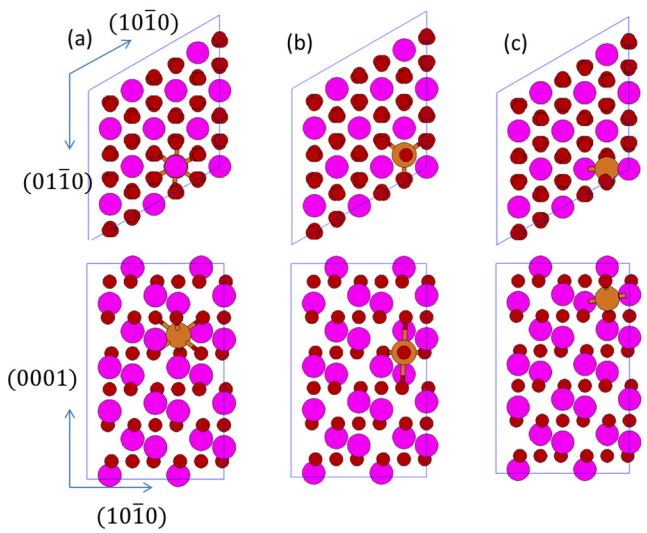


FIG. 7. Three different possible interstitial positions in α-Al_2O_3. Cu atom in (a) has the lowest energy.

APPENDIX B: LDOS ANALYSIS ON ORBITALS

In order to understand the transmission of the filament in α-Al_2O_3 film better, we decompose the contribution to orbitals with different angular momentum along the z-direction and analyze their capability for carrying current. To carry out this analysis, we use the real space orbitals in SIESTA, where p_z and d_{z2} are the $m = 0$ components for p- and d-orbitals, respectively. Since the conductive filament of 3-Cu filament is along (0001) direction, we mainly focus on the central atoms, i.e., Cu-2 and Al-2, which are the bottleneck for conduction. For Cu-2, the LDOS contribution is mainly provided by 4 s, $4p_z$, and $3d_{z2}$ orbitals near the Fermi level as in Fig. 8(a). At the Al-2 atom, the LDOS contribution at the Fermi level is mainly from the 3 s and $3p_z$ orbitals, as shown in Fig. 8(b). That is to say, the $m = 0$ orbitals on the central Cu atom and neighboring Al atoms along the (0001) direction form the conductive path for electrons. Physically, these orbitals contribute the most to

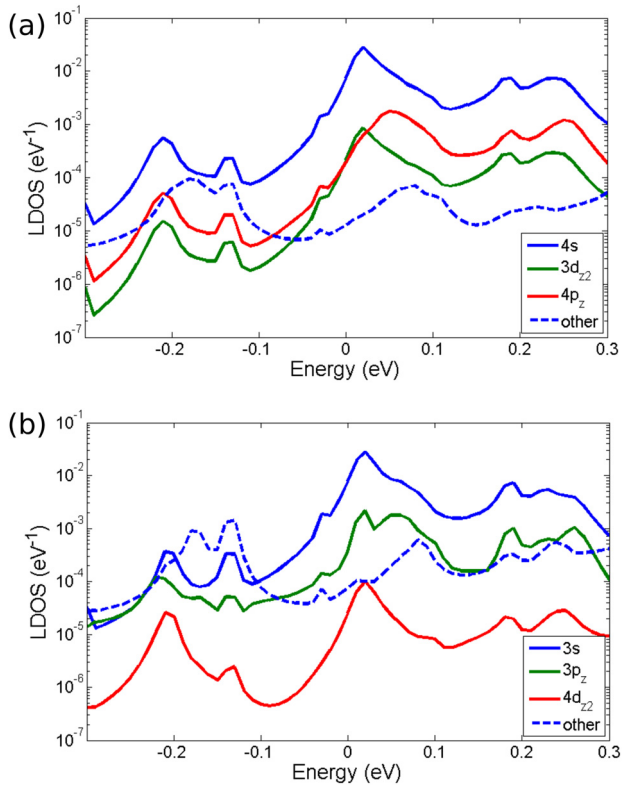


FIG. 8. LDOS on orbitals of the Cu-2 atom (upper) and Al-2 atom (lower) of the 3-Cu atom filament. $m = 0$ orbitals are shown by solid lines and the sum of other orbitals are shown by dashed lines. We find that the $m = 0$ orbitals provide the large LDOS near the Fermi level and form the conductive path in Al and Cu.

[This article is copyrighted as indicated in the article. Reuse of AIP content is subject to the terms at: http://scitation.aip.org/termsconditions. Downloaded to] IP: 128.95.215.214 On: Thu, 06 Nov 2014 19:31:09

current because they are located near the Fermi level and these orbitals are naturally elongated along the transport direction.

[1]A. Chen, S. Haddad, Y. C. Wu *et al.*, Appl. Phys. Lett. **91**, 123517 (2007).
[2]D. C. Kim, S. Seo, S. E. Ahn *et al.*, Appl. Phys. Lett. **88**, 202102 (2006).
[3]T. Fujii, M. Kawasaki, A. Sawa, H. Akoh *et al.*, Appl. Phys. Lett. **86**, 012107 (2004).
[4]X. Guo, C. Schindler, S. Menzel *et al.*, Appl. Phys. Lett. **91**, 133513 (2007).
[5]V. V. Zhirnov, R. K. Cavin III, Stephan Menzel *et al.*, Proc. IEEE **98**, 2185 (2010).
[6]R. Waser, R. Dittmann, G. Staikov, and K. Szot, Adv. Mater. **21**, 2632 (2009).
[7]H. Akinaga and H. Shima, Proc. IEEE **98**, 2237 (2010).
[8]A. Flocke, T. G. Noll, C. Kugeler *et al.*, in *Proc. IEEE Non-Volatile Memory Technology Symposium* (2008), p. 319.
[9]J. J. Yong, M. D. Pickett, X. Li *et al.*, Nat. Nanotechnol. **3**, 429–433 (2008).
[10]D. B. Strukov, G. S. Snider, D. R. Stewart, and R. S. Williams, Nature **453**, 80 (2008).
[11]H. Akinaga, H. Shima, F. Takano, I. H. Inoue, and H. Takagi, IEEJ Trans. Elec. Electron Eng. **2**, 453 (2007).
[12]H.-S. P. Wong, H.-Y. Lee, S. Yu *et al.*, Proc. IEEE **100**, 1951 (2012).
[13]Z. Wang, H. Yu, X. Anh Tran *et al.*, Phys. Rev. B **85**, 195322 (2012).
[14]S. Prada, M. Rosa, L. Giordano *et al.*, Phys. Rev. B **83**, 245314 (2011).
[15]H. Dong Lee, B. Magyari-Köpe, and Y. Nishi, Phys. Rev. B **81**, 193202 (2010).
[16]J. H. Hur, M.-J. Lee, C. Bum Lee *et al.*, Phys. Rev. B **82**, 155321 (2010).
[17]S.-G. Park, B. Magyari-Köpe, and Y. Nishi, Phys. Rev. B **82**, 115109 (2010).
[18]S. Tsui, Y. Y. Xue, N. Das *et al.*, Phys. Rev. B **80**, 165415 (2009).
[19]S. Yu, R. Jeyasingh, Y. Wu, and H.-S. Philip Wong, Phys. Rev. B **85**, 045324 (2012).
[20]J. Son and S. Stemmer, Phys. Rev. B **80**, 035105 (2009).
[21]T. Gu, Z. Wang, T. Tada, and S. Watanabe, J. Appl. Phys. **106**, 103713 (2009).
[22]D. S. Jeong, B. Cheong, and H. Kohlstedt, Solid-State Electron. **63**, 1 (2011).
[23]L. Goux, K. Opsomer, R. Degraeve *et al.*, Appl. Phys. Lett. **99**, 053502 (2011).
[24]L. Goux, K. Opsomer, R. Schuitema *et al.*, in *2011 3rd IEEE International Memory Workshop (IMW)* (2011), p. 1.
[25]L. Goux, K. Opsomer, A. Fraquet *et al.*, Thin Solid Films **533**, 29 (2013).
[26]Y. Wu, S. Yu, B. Lee, and P. Wong, J. Appl. Phys. **110**, 094104 (2011).
[27]L. Chen, H.-Y. Gou, Q.-Q. Sun *et al.*, IEEE Electron Device Lett. **32**(6), 794 (2011).
[28]A. Belmonte, W. Kim, B. T. Chan *et al.*, in *2013 5th IEEE International Memory Workshop (IMW)* (2013),p. 26.
[29]W. Zhu, T. P. Chen, Z. Liu, M. Yang *et al.*, J. Appl. Phys. **106**, 093706 (2009).
[30]Y. Wu, B. Lee, and H.-S. Philip Wong, IEEE Electron. Device Lett. **31**, 1449 (2010).
[31]W. Banerjee, S. Maikap, S. Z. Rahaman *et al.*, J. Electrochem. Soc. **159**(2), H177–H182 (2012).
[32]W. Kim, J. Kim, J. Moon *et al.*, in 2012 4th IEEE International Memory Workshop (IMW) (2012), Vol. 1, p. 20.
[33]H. C. Lin, P. D. Ye, and G. D. Wilk, Solid-State Electron. **50**, 1012 (2006).
[34]D. R. Lide, *CRC Handbook of Chemistry and Physics*, 82nd ed. (CRC Press, Cleverland, OH, 2001).
[35]R. H. French, J. Am. Ceram. Soc. **73**, 477 (1990).
[36]K. Aratani, K. Ohba, T. Mizuguchi *et al.*, Electron Devices Meeting, 2007. IEDM 2007. IEEE International **2007**, 783.
[37]I. G. Batyrev and L. Kleinman, Phys. Rev. B **64**, 033410 (2001).
[38]S. Shi, S. Tanaka, and M. Kohyama, Phys. Rev. B **76**, 075431 (2007).
[39]W. Zhang, J. R. Smith, and A. G. Evans, Acta Mater. **50**, 3803 (2002).
[40]S. V. Eremeev, S. Schmauder, S. Hocker, and S. E. Kulkova, Physica B **404**, 2065 (2009).
[41]J. M. Soler, E. Artacho, J. D. Gale *et al.*, J. Phys. Condensed Matter. **14**, 2745 (2002).
[42]J. P. Perdew, K. Burke, and M. Ernzerhof, Phys. Rev. Lett. **77**, 3865 (1996).
[43]M. Strange, I. S. Kristensen, K. S. Thygesen, and K. W. Jacobsen, J. Chem. Phys. **128**, 114714 (2008).
[44]F. A. Ponce, T. Yamashita, and S. Hahn, Appl. Phys. Lett. **43**, 1051 (1983).

[This article is copyrighted as indicated in the article. Reuse of AIP content is subject to the terms at: http://scitation.aip.org/termsconditions. Downloaded to] IP: 128.95.215.214 On: Thu, 06 Nov 2014 19:31:09